

PHYSICAL REVIEW D

PARTICLES AND FIELDS

THIRD SERIES, VOLUME 43, NUMBER 1

1 JANUARY 1991

RAPID COMMUNICATIONS

Rapid Communications are intended for important new results which deserve accelerated publication, and are therefore given priority in editorial processing and production. A Rapid Communication in Physical Review D should be no longer than five printed pages and must be accompanied by an abstract. Page proofs are sent to authors, but because of the accelerated schedule, publication is generally not delayed for receipt of corrections unless requested by the author.

Experimental bound on the charge radius of the electron neutrino

R. C. Allen,^(a) H. H. Chen,^(b) P. J. Doe,^(c) R. Hausammann,^(d) W. P. Lee,^(e)
X-Q. Lu, H. J. Mahler,^(f) M. E. Potter,^(c) and K. C. Wang^(g)
University of California, Irvine, California 92717

T. J. Bowles, R. L. Burman, R. D. Carlini,^(h) D. R. F. Cochran, J. S. Frank,⁽ⁱ⁾
E. Piasezky,^(j) and V. D. Sandberg
Los Alamos National Laboratory, Los Alamos, New Mexico 87545

D. A. Krakauer^(k) and R. L. Talaga^(k)
University of Maryland, College Park, Maryland 20742
(Received 24 August 1990)

A limit on the electron-neutrino charge radius $|r|$ is derived from a measurement of the weak-neutral-current vector coupling constant g_V obtained in electron-neutrino electron elastic scattering. The 90%-confidence interval for g_V is $-0.177 < g_V < 0.187$, which for $\sin^2\theta_W = 0.227$ implies that the ν_e mean-square charge radius is in the range $-2.74 \times 10^{-32} < \langle r^2 \rangle < 4.88 \times 10^{-32} \text{ cm}^2$, or simply $|r| < 2.2 \times 10^{-16} \text{ cm}$. This is the first experimental bound on the ν_e charge radius, and is the same order of magnitude as bounds for ν_μ structure.

Evidence for electromagnetic interactions of neutrinos would provide an elegant and simple signature of physics beyond that predicted by the minimal standard model. A natural place to seek this evidence is in neutral-current neutrino reactions.¹ The most sensitive searches have concentrated on limits for the two lowest-order electromagnetic moments: namely, the magnetic (dipole) moment and the charge radius of the neutrino. This work reports the first experimental bound on the electron-neutrino charge radius.

In contrast with the neutrino magnetic and electric dipole moments, the neutrino charge radius is not a gauge-invariant quantity.² Nevertheless, an acceptable and measurable neutrino charge-radius form factor has been defined for low- q^2 laboratory interactions.^{3,4} This effective charge radius is defined by the radiative correction to the weak mixing angle measured in neutrino-electron scattering; it is measured as an additive correction to the effective weak-neutral-current vector coupling g_V .⁴ A nonzero charge radius shifts g_V from its un-

corrected value of $g_V = -\frac{1}{2} + 2\sin^2\theta_W$ to $g_V = -\frac{1}{2} + 2(\sin^2\theta_W + \delta)$ where $\sin^2\theta_W$ is the weak mixing angle measured in nonneutrino interactions. The numerical relation of the radiative correction δ to the charge radius is $\delta = (\sqrt{2}\pi\alpha/3G_F)\langle r^2 \rangle = (2.39 \times 10^{30} \text{ cm}^{-2}) \langle r^2 \rangle$. It is important to note that a second convention exists that is equivalent except for a factor of 2 difference in the normalization of $\langle r^2 \rangle$.⁵

The charge radius results in an interference between the weak and electromagnetic interactions, so $\langle r^2 \rangle$ can be either positive or negative. The charge-radius radiative correction is nonzero even in the standard model, due to the contributions from higher-order diagrams involving exchange of Z^0 and W^\pm .^{4,6} DeGrassi, Sirlin, and Marciano⁴ estimate this effective charge radius is $|r| \approx 4 \times 10^{-17} \text{ cm}$ for the electron neutrino. Observation of an anomalous charge radius greater than this could indicate neutrino electromagnetic structure beyond that expected in the minimal standard model.

This experiment measured g_V and searched for evidence

of a neutrino charge radius in $\nu_e e^-$ elastic scattering. A 15-metric-ton tracking calorimeter providing $4.94 \pm 0.07 \times 10^{30}$ target electrons was exposed to $9.16 \pm 0.67 \times 10^{14}$ ν_e/cm^2 from μ^+ decay at rest in the LAMPF beam stop. The neutrino flux also included equal intensities of ν_μ and $\bar{\nu}_\mu$ from π^+ and μ^+ decay. Detailed descriptions of the flux calibration,⁷ the detector,⁸ and the trigger and data analysis⁹ have been published.

The neutrino-electron elastic-scattering signal is obtained from a multiparameter fit to the two-dimensional observed recoil electron angle and energy distributions, assuming contributions from the signal, and cosmic-ray, neutrino-nuclear, and neutron-induced backgrounds.⁹ The observed electron-recoil angular distribution after cosmic-ray and beam-associated backgrounds have been subtracted is shown in Fig. 1. The fitting procedure estimates the elastic-scattering signal to be 295 ± 35 events, as shown by the solid line in Fig. 1. The elastic-scattering rate includes contributions from $\nu_\mu e$ and $\bar{\nu}_\mu e$. As the muon-neutrino and -antineutrino contributions have opposite (anticorrelated) dependence on $\sin^2\theta_W$, the background subtraction of their sum is essentially insensitive to the assumed weak mixing angle. The measured cross sections^{10,11} for muon-neutrino and -antineutrino elastic scattering are used to determine the background contribution of 61 ± 9 events, which is shown as a dashed line in Fig. 1.

There are 234 ± 35 $\nu_e e^- \rightarrow \nu_e e^-$ elastic-scattering events remaining after the subtraction. The experimentally observed $\nu_e e^-$ elastic-scattering rate R depends on the weak-neutral-current couplings (g_V, g_A) through the total cross section and detector acceptance according to

$$R = \kappa \sigma_0 \left\{ \epsilon_L \left[2 + (g_V + g_A)^2 \right] + \frac{1}{3} \epsilon_R (g_V - g_A)^2 \right\}. \quad (1)$$

In expression (1), κ is the product of the integrated neutrino flux and the electron target thickness, $4.53 \pm 0.33 \times 10^{45} \text{ cm}^{-2}$, $\sigma_0 = G_F^2 m_e E_\nu / 2\pi = 1.36 \times 10^{-43}$

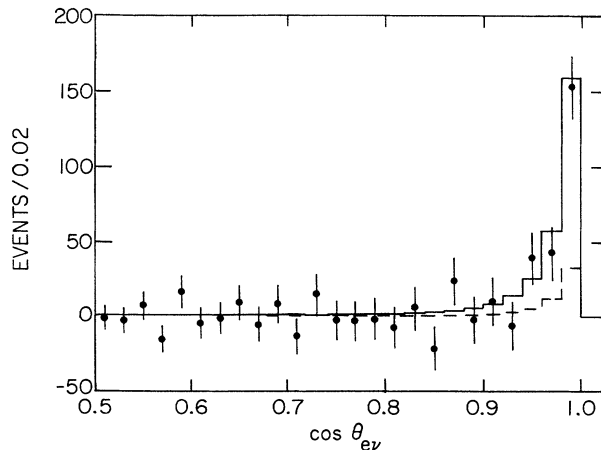


FIG. 1. The angular distribution of recoil electrons after background subtraction. The solid line is the fit result, 295 ± 35 elastic-scattering events. The dashed line is the contribution from $61 (\nu_\mu + \bar{\nu}_\mu) e$ events.

cm^2 , and $\epsilon_{L,R}$ are the spectrum-averaged detection efficiencies for left-handed or right-handed recoil electrons, respectively.¹² The detection efficiencies, averaged over the neutrino flux, are evaluated by a Monte Carlo simulation to be $\epsilon_L = 0.167 \pm 0.009$ and $\epsilon_R = 0.037 \pm 0.002$.

After replacing g_A by its standard-model value, $g_A = -\frac{1}{2}$, Eq. (1) can be reexpressed as a quadratic equation for g_V :

$$0 = (\epsilon_L + \frac{1}{3} \epsilon_R) g_V^2 + (\frac{7}{2} \epsilon_L + \frac{1}{3} \epsilon_R) g_V + \left[(\frac{9}{4} \epsilon_L + \frac{1}{12} \epsilon_R) - \frac{R}{\kappa \sigma_0} \right], \quad (2)$$

which is solved as $g_V = 0.003$. A Monte Carlo method is used to establish confidence intervals for g_V . Equation (2) is solved for g_V while allowing the uncorrelated quantities R , κ , and ϵ to independently fluctuate (with Gaussian widths of 15.0%, 7.4%, and 5.0%, respectively) about their central values. Figure 2 shows the resulting distribution for 10^6 trials. If $P(V)$ is the probability of obtaining $g_V = V$ with this method, the 90%-confidence region is defined such that the lower limit (LL) and upper limit (UL) satisfy

$$\int_{\text{LL}}^{0.003} P(V) dV = \int_{0.003}^{\text{UL}} P(V) dV = 0.45.$$

The 90%-confidence interval measured by this experiment $-0.177 < g_V < 0.187$ is delimited by the dashed lines in Fig. 2. The present world data for the masses of the W^\pm and Z^0 yield $\sin^2\theta_W = 0.227$;¹³ thus, the vector coupling without radiative corrections is $g_V = -0.046$. Comparison of that value with the measured confidence interval from this experiment shows that the radiative correction defined in the second paragraph is in the range $-0.131 < 2\delta < 0.233$. This leads immediately to the lim-

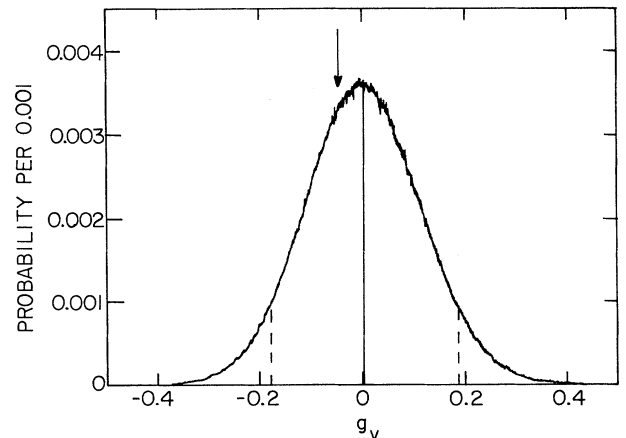


FIG. 2. Probability distribution for g_V measured by the Monte Carlo method described in the text. The central value is indicated by a solid line, the 90%-confidence interval is between the dashed lines. The standard-model prediction for $\sin^2\theta_W = 0.227$, $g_V = -0.046$ is shown by the inverted arrow.

its

$$-2.74 \times 10^{-32} < \langle r^2 \rangle < 4.88 \times 10^{-32} \text{ cm}^2 \text{ (90\% C.L.)} \quad (3)$$

Thus, the ν_e charge radius is $|r| < 2.2 \times 10^{-16}$ with 90% confidence, which represents a new upper bound on the dimensions of internal structure of the electron neutrino. This result can also be interpreted directly as an upper limit against a possible ν_e anapole moment. The limits obtained here for the electron neutrino are comparable to the bounds on the muon-neutrino charge radius set separately by the Brookhaven experiment¹⁰ ($-2.81 \times 10^{-32} < \langle r^2 \rangle < 0.51 \times 10^{-32} \text{ cm}^2$, see Ref. 14) and by the CHARM Collaboration¹¹ ($-2.70 \times 10^{-32} < \langle r^2 \rangle < 2.11 \times 10^{-32} \text{ cm}^2$, see Ref. 15). Although these results provide an upper bound on possible internal dimensions of the neutrino, an order of magnitude improvement in the experimental precision for g_V is necessary to allow

direct tests of the radiative-correction scheme in the standard model.

The success of this experiment was due in large part to the technical contributions of N. Briscoe, R. S. DeLay, J. Sena, and T. N. Thompson, as well as the excellent beam quality and support at LAMPF. We acknowledge enlightening conversations with M. V. Diwan and R. E. Lanou concerning previous experimental results for muon neutrinos, and with W. J. Marciano and J. D. Vergados regarding theoretical aspects and definitions of the neutrino charge radius. We thank A. B. Wickland for providing vector-boson mass-fitting programs and preliminary Collider Detector at Fermilab results. This work was paid for, in part, by the National Science Foundation and the U. S. Department of Energy.

^(a)Now at Hewlett Packard Laboratories, Palo Alto, CA 94304.

^(b)Deceased.

^(c)Now at Los Alamos National Laboratory, Los Alamos, NM 87545.

^(d)Now at LeCroy SA, CH 1217, Meyrin 1, Geneva, Switzerland.

^(e)Now at Jet Propulsion Laboratory, Pasadena, CA 91109.

^(f)Now at Cerebus AG, Geneva, Switzerland.

^(g)Now at Rockwell International, Thousand Oaks, CA 91360.

^(h)Now at Continuous Electron Beam Accelerator Facility, Newport News, VA 23606.

⁽ⁱ⁾Now at Brookhaven National Laboratory, Upton, NY 11973.

^(j)Permanent address: Physics Department, Tel Aviv University, Ramat Aviv, Israel.

^(k)Now at Argonne National Laboratory, Argonne, IL 60439.

¹J. E. Kim, V. Mathur, and S. Okubo, Phys. Rev. D **9**, 3050 (1974).

²Robert E. Schrock, Nucl. Phys. **B206**, 359 (1982); Benjamin W. Lee and Robert E. Schrock, Phys. Rev. D **16**, 1444 (1977).

³J. L. Lucio, A. Rosado, and A. Zapeda, Phys. Rev. D **31**, 1091 (1985).

⁴G. DeGrassi, A. Sirlin, and W. J. Marciano, Phys. Rev. D **39**, 287 (1989).

⁵For both conventions, the charge radius is defined in terms of an electromagnetic form factor $f(q^2)$ as $\langle r^2 \rangle = 6\delta f(q^2) / \partial q^2|_{q^2=0}$. We choose a definition and normalization common in the literature, for instance Ref. 10, where $f(q^2)$ is defined according to $\langle \bar{\nu} | j_\mu^\nu | \nu \rangle = f(q^2) \bar{u}_\nu \gamma^\mu u_\nu$. An alternative convention, published in Ref. 4, equates the same matrix element to $f(q^2) \bar{u}_\nu \gamma^\mu \frac{1}{2} (1 - \gamma_5) u_\nu$. For equal shifts δ of the vector coupling constant, this latter convention requires a charge radius $\langle r^2 \rangle$ that is twice as large compared to the definition used

in this article.

⁶J. E. Kim, Phys. Rev. D **14**, 3000 (1976).

⁷R. C. Allen *et al.*, Nucl. Instrum. Methods Phys. Res. Sect. A **284**, 347 (1989); R. L. Burman, M. E. Potter, and E. S. Smith, Nucl. Instrum. Methods Phys. Res. Sect. A **291**, 621 (1990).

⁸R. C. Allen *et al.*, Nucl. Instrum. Methods Phys. Res. Sect. A **269**, 177 (1988).

⁹R. C. Allen *et al.*, Phys. Rev. Lett. **64**, 1330 (1990).

¹⁰L. A. Ahrens *et al.*, Phys. Rev. D **41**, 3301 (1990).

¹¹J. Dorenbosch *et al.*, Z. Phys. C **41**, 567 (1989).

¹²This separates the uniform and $(1 - \cos\theta)^2$ contributions to the differential cross section in the center of mass.

¹³Based on $M_W = 80.166 \pm 0.296$ GeV, $M_Z = 91.161 \pm 0.030$ GeV obtained from a combined fit to all presently available W^\pm - and Z-boson mass data (central values for each datum given in GeV): UA2 Collaboration, J. Alitti *et al.*, Phys. Lett. **B 241**, 150 (1990) ($M_W = 80.79$); CDF Collaboration, F. Abe *et al.*, Phys. Rev. Lett. **65**, 2243 (1990) ($M_W = 79.91$); Particle Data Group, J. J. Hernandez *et al.*, Phys. Lett. **B 239**, 1 (1990) ($M_Z = 91.161$).

¹⁴The numerical constant relating δ to $\langle r^2 \rangle$ published in Ref. 10 was apparently evaluated with an inconsistent value for G_F resulting in charge-radius limits that were too small by a factor of $\sqrt{2}$. The muon-neutrino limits quoted here use the more recent W/Z mass measurement of Ref. 13 to determine $\sin^2\theta_W$ and so differ slightly from the corrected values obtained from Ref. 10.

¹⁵The 90%-confidence interval ($\pm 1.64\sigma$) for g_V from Ref. 11 is $-0.136 < g_V < 0.101$. The $\langle r^2 \rangle$ limit quoted here is based on the present δ -to- $\langle r^2 \rangle$ conversion factor, and the updated $\sin^2\theta_W$, and so differs somewhat from the value found in Ref. 11.